

UNITED STATES PATENT AND TRADEMARK OFFICE

BEFORE THE PATENT TRIAL AND APPEAL BOARD

PANASONIC SYSTEM NETWORKS CO., LTD.
Petitioner

v.

6115187 CANADA, INC.
Patent Owner

Case IPR _____
U.S. Patent No. 6,844,990
Issue Date: January 18, 2005

Title: METHOD FOR CAPTURING AND DISPLAYING A
VARIABLE RESOLUTION DIGITAL PANORAMIC IMAGE

DECLARATION OF SHISHIR K. SHAH, PH.D.

I, Shishir K. Shah, declare as follows:

1. I have been retained by Panasonic System Networks Co., Ltd. (“Petitioner”) as an expert in this case.
2. I have been asked to provide my opinions concerning the subject matter disclosed in U.S. Patent No. 6,844,990 (“the ‘990 patent”) and in the prior art, in particular relating to image correction methods.
3. I have also been asked to provide my opinions concerning the state of the relevant art prior to May 11, 2001, and the level and knowledge of one of ordinary skill in the art in the May 2001 time frame.
4. I have reviewed certain prior art references and analyzed whether certain limitations of the claims of the '990 patent are disclosed and/or would have been obvious in view of those prior art references. I have also reviewed portions of the Declaration of Jack Feinberg, Ph.D. (Exhibit 1013).
5. My opinions set forth in this declaration are based on my education, training and experience in the relevant field, as well as the materials I reviewed in this case, and the scientific knowledge regarding the same subject matter.

I. Qualifications

6. I earned a bachelor of science (B.S.) in Mechanical Engineering from the University of Texas at Austin in 1994, a master of science (M.S.) in Electrical and Computer Engineering from the University of Texas at Austin in 1995, and a

Ph.D. in Electrical and Computer Engineering from the University of Texas at Austin in 1998.

7. I have over 20 years of experience of in the areas of imaging and image analysis.

8. I am currently an Associate Professor in the Department of Computer Science at the University of Houston.

9. I am currently serving as the Director of the Quantitative Imaging Lab in the Department of Computer Science at the University of Houston.

10. A listing of my publications and research is included in my curriculum vitae, a copy of which is attached as Appendix A.

11. I have been retained in this matter by Panasonic System Networks Co., Ltd. (“Petitioner”) to provide an analysis of the scope and content of prior art references that existed prior to the earliest date of filing of the patent application underlying U.S. Patent No. 6,844,990 (“the ‘990 patent”). In particular, I analyzed whether certain limitations of the claims of the ‘990 patent are described in the prior art references.

12. I am being compensated for my work. My fee is not contingent on the outcome of any matter or on any of the technical positions I explain in this declaration. I have no financial interest in Petitioner.

13. I have been informed that the assignee of the patent, 6115187 CANADA, INC., is also known as ImmerVision Inc. (hereinafter referred to as “Patentee”). I have no financial interest in the Patentee or the ‘990 patent.

II. Documents Reviewed

14. I have reviewed the ‘990 patent. Exhibit 1001.

15. I have reviewed European Patent Publication EP 1 028 389 A2 Shiota (“Shiota”). Exhibit 1008.

16. I have reviewed an English language translation of Japanese Patent Application Publication No. 2000-242773 to Matsui (“Matsui”). Exhibit 1010. I have also looked at the original Japanese document. Exhibit 1009.

17. I have reviewed an English language translation of Japanese Patent Application Publication No. 11-261868 to Enami (“Enami”). Exhibit 1012. I have also looked at the original Japanese document. Exhibit 1011.

18. I have also reviewed U.S. Patent No. 5,686,957 (“Baker”) (Exhibit 1002,), U.S. Patent No. 6,128,145 (“Nagaoka”)(Exhibit 1003,), and U.S. Patent No. 3,953,111 (“Fisher”)(Exhibit 1004).

19. As noted earlier, I have also reviewed portions of the Declaration of Jack Feinberg, Ph.D. Exhibit 1013.

III. The Person of Ordinary Skill in the Relevant Field in the Relevant Timeframe

20. I have been informed that “a person of ordinary skill in the relevant art” is a hypothetical person to whom an expert in the relevant field could assign a routine task with reasonable confidence that the task would be successfully carried out. I have been informed that the level of skill in the art can be deduced by examining the prior art references. I have been informed that "a person of ordinary skill in the relevant art" is a hypothetical person who is presumed to have known the relevant art at the time of the invention. Factors that may be considered in determining the level of ordinary skill in the art may include: (1) type of problems encountered in the art; (2) prior art solutions to those problems; (3) rapidity with which innovations are made; (4) sophistication of the technology; and (5) educational level of active workers in the field. In a given case, every factor may not be present, and one or more factors may predominate. In many cases a person of ordinary skill will be able to fit the teachings of multiple patents together like pieces of a puzzle.

21. I have been informed that the date for determining whether a document or information is considered “prior art” is May 11, 2001.

22. A person of ordinary skill in the subject matter claimed and disclosed in the ‘990 patent would have at least a bachelor’s degree in Physics and/or Electrical

Engineering and at least five years' experience working with lenses or related optical systems.

23. The prior art discussed herein demonstrates that a person of ordinary skill in the relevant art, before May 11, 2001, would have been aware of panoramic objective lenses, fish-eye lenses and other wide-angle lenses.

24. A person of ordinary skill in the relevant art would have been aware of panoramic objective lenses with non-linear distribution functions, *i.e.*, a distribution function of image points that is not linear relative to the field angle of the object points of the panorama.

25. A person of ordinary skill in the relevant art would also have understood the desirability of, and how to, correct an image obtained from a panoramic objective lens having a non-linear distribution function, including by means of a reciprocal function of the non-linear distribution function and by means of the non-linear distribution function.

26. Based on my education and experience, I have a very good understanding of the capabilities of a person of ordinary skill in the relevant art at the time of invention.

IV. Background of the Technology

27. It was well known prior to May 2001 that certain fish-eye lenses produced highly distorted images. Such an image could be captured using a CCD

or other electronic camera device, and the captured image could be corrected using a computer.

28. In 1994, I was lead author on a paper entitled: "A Simple Calibration Procedure for Fish-Eye (High Distortion) Lens Camera*." This paper was published in 1994 in the IEEE Proceedings of the International Conference on Robotics and Automation, Vol. 4, pp. 3422-3427.

29. In this paper, it was shown that a fish-eye lens had a non-linear distribution function and that such function could be estimated using a calibration pattern. I discussed a new algorithm for the geometric camera calibration of a fish-eye lens mounted on a CCD TV camera. The algorithm determined a mapping between points in the world coordinate system and their corresponding point locations in the image plane. Specifically, a non-linear distortion model was developed that would relate the points on an imaged object to its corresponding points on the image plane and the algorithm discussed allowed the estimation of the coefficient of the non-linear distortion model. Further, a method for correcting the obtained fish-eye image was presented that used an inverse mapping by traversing points in the corrected image and finding corresponding points in the fish-eye image so that the intensity values or image color could be interpolated and mapped to the corrected image. Finally, this paper shows that the corrected image

resulted in a number of pixels that are greater than the fish-eye image due to expanded number of pixels from the periphery of the fish-eye image.

30. In 1996, I was lead author on another paper, entitled: “Intrinsic Parameter Calibration Procedure For A (High-Distortion) Fish-Eye Lens Camera With Distortion Model And Accuracy Estimation.” This paper was published in the journal *Pattern Recognition*, Vol. 29, No. 11, pp. 1775-1788.

31. This paper expanded on the work presented in the paper in 1994 and discussed a non-linear distortion correction model addressing both radial and tangential distortions. Further, inverse mapping was also discussed to ensure that every pixel intensity was mapped in the expanded corrected image while using the estimated distortion coefficients in correcting the distorted image.

32. Further, as explained in the Declaration of Jack Feinberg, Ph.D. (Exhibit 1013,), U.S. Patent No. 5,686,957 (“Baker”) (Exhibit 1002,), U.S. Patent No. 6,128,145 (“Nagaoka”)(Exhibit 1003,), and U.S. Patent No. 3,953,111 (“Fisher”)(Exhibit 1004) demonstrate that panoramic objective lenses having an image point distribution function that is not linear relative to the field angle of object points of the panorama, the distribution function having a maximum divergence of at least $\pm 10\%$ compared to a linear distribution function, such that the panoramic image obtained has at least one substantially expanded zone and at

least one substantially compressed zone, were well known to persons of ordinary skill in the art prior to May 2001.

V. The ‘990 Patent

33. The ‘990 patent discloses panoramic objective lenses having non-linear distribution functions of image points, and methods for correcting the non-linearity of the initial image.

34. The ‘990 patent discloses two embodiments of correction methods. Exhibit 1001, ‘990 patent, col. 10, line 6 – col. 14, line 41.

35. The first disclosed embodiment “involves correcting the initial image by means of a function Fd^{-1} that is the reciprocal function of the distribution function Fd according to the present invention. As the distribution function Fd is known and determined at the time the non-linear objective lens is designed, it is easy to deduce the reciprocal function Fd^{-1} therefrom. This correction step allows a corrected image to be obtained in which the non-linearity due to the objective lens according to the present invention is removed. The corrected image is equivalent to an image taken by means of a classical panoramic objective lens and can then be processed by any classical display software program available in stores, provided for transferring the image points of an image disk into a three-dimensional space and for interactively displaying a sector of the image obtained.” Exhibit 1001, ‘990 patent, col.10, lines 39-53.

36. The '990 patent states that the "second alternative of the method involves using the distribution function F_d in an image display algorithm working backwards, that is defining in real time the color of the pixels of a display window using the image points of the image disk." Exhibit 1001, '990 patent, col. 10, lines 54-58.

37. Claim 10 of the '990 patent states:

A method for displaying an initial panoramic image obtained in accordance with the method according to claim 1, the method for displaying comprising: correcting the non-linearity of the initial image, performed by means of a reciprocal function of the non-linear distribution function of the objective lens or by means of the non-linear distribution function.

38. Claim 11 of the '990 patent states:

The method according to claim 10, wherein the step of correcting comprises a step of transforming the initial image into a corrected digital image comprising a number of image points higher than the number of pixels that the image sensor comprises.

39. Claim 15 of the '990 patent states:

The method according to claim 10, further comprising: determining the color of image points of a display window, by projecting the image points of the display window onto the initial image by means of the non-linear distribution function, and allocating to each image point

of the display window the color of an image point that is the closest on the initial image.

40. Claim 16 of the '990 patent states:

The method according to claim 15, wherein the projection of the image points of the display window onto the initial image comprises: projecting the image points of the display window onto a sphere or a sphere portion, determining the angle in relation to the center of the sphere or the sphere portion of each projected image point, and projecting onto the initial image each image point projected onto the sphere or the sphere portion, the projection being performed by means of the non-linear distribution function considering the field angle that each point to be projected has in relation to the center of the sphere or the sphere portion.

VI. Claim Interpretation

41. In reviewing the claims of the '990 patent, I understand that the claims are generally accorded their broadest reasonable interpretation in light of the patent specification, and should be free from any limitations disclosed in the specifications that are not expressly listed in the claims.

42. I also understand that claimed terms should be accorded their ordinary and accustomed meaning unless the specification otherwise defines the terms.

43. In my analysis, I have construed the terms stated in the claims relating to corrections using their ordinary and accustomed meaning, which would be the broadest reasonable interpretation in light of the patent specification.

VII. Shiota

44. I have been informed that Shiota (Exhibit 1008) published August 16, 2000, and that it is prior art to the '990 patent.

45. Shiota discloses an image transformation system for correcting the output from a non-linear objective fish-eye lens.

46. Shiota discloses a fisheye lens 2 attached to a CCD camera 1. Exhibit 1008, [0044] and Fig. 4.

47. Shiota discloses that when the focal distance of the fisheye lens is f , the nonlinear stereographic projection $h=2f \cdot \tan(\theta/2)$ is established. Exhibit 1008, [0037].

48. Shiota discloses the method of transforming the fish-eye image into a planar image where the planar image is obtained by projecting points from the hemispherical objective lens surface onto a plane intersecting the lens surface at a point identifying the viewing direction from the origin of the camera. Exhibit 1008, [0028-0032].

49. Shiota discloses that the pixels on the fish-eye image are related to points projected onto the lens surface according to the nonlinear lens projection

$h=2f \cdot \tan(\theta/2)$ and that this relationship is used in relating pixels of the fish-eye image to the planar image. Knowing the lens projection, the pixels on the fish-eye image can be related to points on the lens surface (Fig. 1) and can be computed according to the nonlinear distribution function of the lens. Exhibit 1008, [0033-0041].

50. Shiota further discloses that generating the planar image requires that the points on the lens surface be mapped to a plane intersecting the lens surface, such mapping being defined by arithmetic calculations based on underlying trigonometric geometry. Exhibit 1008, [0028-0032].

51. Shiota discloses a transformation where the mapping of points between the planar image and the lens surface are computed separately from the mapping of points between the lens surface and the fish-eye image. Exhibit 1008, [0028 and 0033].

52. Shiota thus discloses a two step process of transforming the image obtained by a non-linear objective fish-eye lens into an undistorted image. Exhibit 1008, [0028-0042].

53. Shiota discloses that the fish-eye image obtained is related to the spherical objective fish-eye lens according to the nonlinear stereographic projection $h=2f \cdot \tan(\theta/2)$ is established. Exhibit 1008, [0037].

54. Shiota discloses a first coordinate calculating unit for obtaining first projection coordinates derived by projecting coordinates on the plane image onto a fisheye image face as an imaginary object face, and a second coordinate calculating unit for obtaining second projection coordinates derived by projecting the first projection coordinates obtained by the first coordinate calculating unit onto the fisheye image face. Exhibit 1008, [0001, 0009-0010].

55. More specifically, Shiota discloses an operation part 40 comprising a first coordinate calculating unit 35, a second coordinate calculating unit 36, a first lookup table 37 connected to the first coordinate calculating unit 35, and a second lookup table 38 connected to the second coordinate calculating unit 36. The first coordinate calculating unit 35 is a part of executing the calculation of the first step shown in FIG. 3 and can obtain the first projection coordinates (X_2, Y_2, Z_2) on the hemispherical face from the (u, v) coordinates in the plane image. This relates the point on the planar image to the lens surface. The first lookup table 37 is a table for obtaining the correction coefficient k_1 from the distance L . Exhibit 1008, [0045] and Fig. 4.

56. Additionally, Shiota discloses that the second coordinate calculating unit 36 is a part of executing the calculation of the second step in FIG. 3 and can obtain the second projection coordinates (p_1, q_1) on the fisheye image face from the first projection coordinates (X_2, Y_2, Z_2) derived by the first coordinate calculating

unit 35. This relates the point on the lens surface to the pixel on the fish-eye image. The second lookup table 38 is a table for obtaining the correction coefficient k_2 . Exhibit 1008, [0046].

57. Shiota discloses a correction coefficient k_2 , which equals the function h over the radius r . *i.e.*, where r is the distance from the origin to the projected point. Shiota further discloses that h can equal $2f \cdot \tan(\theta/2)$. Accordingly, when $h=2f \cdot \tan(\theta/2)$, the correction coefficient k_2 is based on a non-linear distribution function. Exhibit 1008, [0037-0041].

58. Shiota discloses “transforming a fisheye image obtained using a fisheye lens (2) into a plane image for display comprising: a first coordinate calculating unit (35) for obtaining first projection coordinates derived by projecting coordinates on the plane image onto a fisheye face as an imaginary object face.” Exhibit 1008, Abstract.

59. Shiota discloses “Necessary parameters are, as shown in Figs. 1 and 2, (X_0, Y_0, Z_0) indicative of the center (origin) of a plane image and change amounts $\partial u_x, \partial v_x, \partial u_y, \partial v_y, \partial u_z, \partial v_z$ in the respective axes of the (X, Y, Z) coordinates when a point is moved in the respective directions on the (u, v) coordinate system by an amount of one pixel (corresponding to one pixel on the monitor screen).” Exhibit 1008 [0025]. “The parameters can be easily obtained from the information of the angle information (ψ, θ, α) of the view point and the magnification of the

image.” Exhibit 1008 [0026]. Since point P’ “is on the surface of the hemisphere of radius of 1, the zenithal angle (θ_1) is unconditionally determined ...” Exhibit 1008, [0034].

60. Shiota discloses “First, the coordinates of a point P’ (first projection coordinates) on the hemispherical face as an imaginary object face, which is a projection of a point P on a plane image (the u, v coordinates) are obtained.” Exhibit 1008, [0028].

61. Shiota discloses, as a second step of the calculation, “a procedure of obtaining second projection coordinates $w(p1, q1,)$ on a fisheye image face from the first projection coordinates ($X2, Y2, Z2$) determined (refer to FIG. 1 with respect to w) will be explained.” Exhibit 1008, [0033].

62. An example of a specific function of $F(\theta_1)$ according to the projecting method is the stereographic projection, which has the non-linear distribution function: $2f \cdot \tan(\theta/2)$. Exhibit 1008, [0037].

VIII. Matsui

63. I have been informed that Matsui (Exhibit 1009) was published on September 8, 2000 and that it is prior art to the ‘990 patent.

64. Matsui discloses a data image conversion device, in which image data obtained with a fish-eye lens is corrected to remove distortion so that it may be displayed. Exhibit 1010, [0001].

65. Matsui discloses that a camera 1 uses a fish-eye lens 11 that is capable of image capture at a field angle of 90° or more with respect to the optical axis. Exhibit 1010, [0017].

66. Matsui discloses that the fish-eye lens includes the property $h=2f\cdot\tan(\theta/2)$. As a result, the amount of information in the area of a large field angle, the periphery of a circular image, is increased. Exhibit 1010, [0017].

67. More specifically, Matsui discloses the calculation of pixel positions on the circular surface from the pixel positions actually captured by the CCD utilizing the non-linear distribution function $h = 2f\cdot\tan(\theta/2)$. Exhibit 1010, [0025]

68. Matsui discloses a data converter 2 that is an image data conversion device that converts circular image data stored in a first image memory 3 into cylindrical image data using a conversion process. Then, the data converter 2 outputs the image data to a second image memory. Exhibit 1010, [0018].

69. Matsui discloses that the circular image obtained by the fish-eye lens can include an image of all orientations, but the image becomes more distorted further toward an outer periphery. Exhibit 1010, [0003].

70. Matsui further discloses that this distortion can be largely removed from the circular image data by mapping the points in the circular image to points onto a hemisphere surface. Further, the image data mapped onto a hemisphere surface can be further projected onto a planar surface. Exhibit 1010, [0003].

71. Matsui discloses that circular image data obtained by images captured using a fish-eye lens can be mapped onto a cylindrical surface by considering points in the circular image indexed by $(g(\Theta) \cdot \cos\psi, g(\Theta) \cdot \sin\psi)$, such that the origin of the indexing is at the center of the circular image and where Θ is a parameter fulfilling $0 < \Theta < \pi/2$; $g(\Theta)$ being a function fulfilling $g(0) = 0$ and monotonically increasing in the range of Θ ; and ψ being an angle formed by a line segment joining the center and a point on the circular image. The points so indexed are mapped onto the cylindrical surface indexed by $(R, \psi, R/\tan\Theta)$ where R is a constant. Exhibit 1010, [0006].

72. Matsui further discloses that $g(\Theta)$ in the indexing of the circular image points can be the distance of each point on the circular image computed from the center of the circular image, and as such, according to the mapping, a line segment oriented in a radial direction from the center of the circular image data, where the radial direction is given by ψ , is converted into the cylindrical coordinate system where R is a constant (i.e., as a line segment oriented from up to down on a cylindrical surface of radius R). This results in mapping each line from the circular image to a segment on the cylindrical surface, thereby expanding the line and correcting the distortion. The image converted into a cylindrical surface can be readily made into a planar image by projecting the cylindrical surface. Exhibit 1010, [0008].

73. Matsui discloses that when using a lens having the property $h = g(\theta)$ (h being an image height and θ being a field angle), an amount that $g(\theta)$ increases accompanying an increase of θ is the same as the amount that the image height h increases. In such a case, the circular image is converted into an ideal, undistorted hemisphere surface. Hence the mapping of the circular image to the cylindrical surface to remove the distortion uses the lens distribution function. Exhibit 1010, [0009].

74. More specifically, Matsui discloses that a point on the circular image can be indexed by $(h \cdot \cos \psi, h \cdot \sin \psi)$, where h is the distance from the center of the circular image and ψ is the angle of the line segment that links the point to the center of the circular image (Fig. 3). Considering the lens distribution $h = 2f \cdot \tan(\theta/2)$, the point is indexed by $(2f \cdot \tan(\theta/2) \cdot \cos \psi, 2f \cdot \tan(\theta/2) \cdot \sin \psi)$. This point mapped to the cylindrical surface of radius R and $z = R/\tan \theta$ is given as $(R, \psi, R / \tan \theta)$. Exhibit 1010, [0023].

75. Matsui discloses that points in the circular image can be directly referenced by indexing ψ and z of the cylindrical coordinates according to the relationship $(2f \cdot R \cdot \cos \psi / \{(R^2 + z^2)^{1/2} + z\}, 2f \cdot R \cdot \sin \psi / \{(R^2 + z^2)^{1/2} + z\})$ derived by using the trigonometric expansion $h = 2f \cdot \tan(\theta/2) = 2f \cdot \{\sin \theta / (1 + \cos \theta)\}$. Exhibit 1010, [0025]. This provides an unambiguous determination as to which

pixel position of the cylindrical surface each pixel of the circular image is transformed into.

76. Matsui also discloses that rather than using the lens distribution function $h = g(\theta)$, an inverse function $\theta = \tan^{-1}(R/z)$ can be used to relate points on the cylindrical surface to the points in the circular image. In this case, the points in the circular image can be directly referenced by indexing ψ and z of the cylindrical coordinates according to the relationship $(f \cdot G(\tan^{-1}(R/z))) \cdot \cos\psi$, $f \cdot G(\tan^{-1}(R/z)) \cdot \sin\psi$. Exhibit 1010, [0030-0031].

77. Matsui discloses that $h = 2f \cdot \tan(\theta/2) = 2f \cdot \{\sin\theta/(1 + \cos\theta)\}$. Exhibit 1010, [0025].

78. Matsui discloses a data converter 2 that calculates the circular surface S pixel position corresponding to each pixel on the post-conversion cylindrical surface C, then converts the pixel data of the pixel positions as respective pixel data on the cylindrical surface C. As a result, as shown in Fig. 4, the pixel data on the circular surface S is converted as respective pixel data on the cylindrical surface C. Exhibit 1010, [0026].

79. The data converter 2 converts P1 shown in Fig. 3 into P2 shown in Fig. 2. Exhibit 1010, [0023]. Matsui discloses correcting the non-linearity of the initial image by means of the non-linear distribution function. Specifically, Matsui discloses that rather than using the lens distribution function $h = g(\theta)$, an inverse

function $\theta = \tan^{-1} (R / z)$ can be used to relate points on the cylindrical surface to the points in the circular image. In this case, the points in the circular image can be directly referenced by indexing ψ and z of the cylindrical coordinates according to the relationship $(f \cdot G(\tan^{-1} (R / z)) \cdot \cos \psi, f \cdot G(\tan^{-1} (R / z)) \cdot \sin \psi)$. Exhibit 1010, [0030-0031].

80. Matsui expands the edges of the image, and thereby transforms the initial image into a corrected digital image where the number of image points is higher than the number of pixels that the image sensor comprises.

IX. Enami

81. I have been informed that Enami (Exhibit 1011) published on September 24, 1999 and that it is prior art to the '990 patent.

82. Enami discloses a fisheye lens camera, including a non-linear image distortion correction method. Exhibit 1012, Abstract.

83. Enami discloses that an image captured by a fisheye lens 1-1 and a CCD imaging device 1-2 is stored in a picture member 1-3, and an image correction processing unit 1-4 operates coordinate transform for correcting an installation angle of a fisheye lens camera and coordinate transform for correcting distortion of a fisheye lens image of equal area projection is transformed through mapping at high speed. Exhibit 1012, Abstract.

84. Enami discloses that an image correction processing circuit 13-4 corrects a distorted image of the fisheye lens so as to recover an original image with respect to a monitor display region, and the corrected picture image (NTSC) output circuit 13-5 outputs the corrected image signal as a normal television picture signal of an NTSC format. Exhibit 1012, [0007].

85. Enami discloses that a frame corresponding to a displayed frame is assumed as the virtual image frame 14-1. Exhibit 1012, [0017].

86. Enami discloses that an image obtained using a fish-eye lens is a mapping of image incident from a specific direction (r, θ, ϕ) to a point (x'', y'') expressed by the transform $x'' = L\cos\theta$ and $y'' = L\sin\theta$, where L is the image height and is dependent on the lens projection or the lens distribution function. Exhibit 1012, [0053-0056].

87. Enami discloses that using the mapping, a coordinate of a point in the fisheye lens image corresponds to a coordinate of a point arranged on a raster in a corrected image, and that a color information signal of the point having the corresponding coordinates is made to correspond. Exhibit 1012, [0058].

88. Enami discloses that to obtain a smooth corrected image, linear interpolation of the color information can be used. Exhibit 1012, [0072-74]. In doing so, Enami describes calculation of the color value of a coordinate point on the fisheye lens image by converting mapped coordinate points to integers by

omitting the decimal points, or rounding down, and utilizing the color values at the corresponding integer coordinate points. Similarly, rounding up to obtain another integer coordinate is also described. Finally, the use of both integer coordinates is described as part of linear interpolation. It is well understood that interpolation can be used to obtain a smoother color value and multiple approaches can be utilized in determining the calculation of the color value. Enami discloses the usage of both the rounding up and rounding down process in order to find the closest coordinate point. Enami further discloses the averaging of the rounding up and rounding down processes in order to find the closest coordinate point and to obtain a smoother color value. Exhibit 1012, [0072-0074].

89. Enami discloses that a relationship between a point (x,y) in the fisheye lens imaging plane 14-3 and a point (p,q) in the image frame 14-1 is expressed by a relation of Equation (1):

$$\left. \begin{aligned} x &= \frac{R\{pA - qB + mR \sin \phi \sin \theta\}}{\sqrt{p^2 + q^2 + m^2 R^2}} \\ y &= \frac{R\{pC - qD + mR \sin \phi \sin \theta\}}{\sqrt{p^2 + q^2 + m^2 R^2}} \\ A &= (\cos \omega \cos \theta - \sin \omega \sin \theta \cos \phi) \\ B &= (\sin \omega \cos \theta + \cos \omega \sin \theta \cos \phi) \\ C &= (\cos \omega \sin \theta + \sin \omega \cos \theta \cos \phi) \\ D &= (\sin \omega \sin \theta - \cos \omega \cos \theta \cos \phi) \end{aligned} \right\}$$

Exhibit 1012, [0019-0020].

90. Enami discloses that a distortion of the fisheye lens image is corrected using the relationship of Equation (1) so as to recover the original image for display on a monitor. Exhibit 1012, [0021].

91. Enami discloses that the image correction processing circuit 13-4 obtains the point (x,y) in the fisheye lens imaging plane 14-3 corresponding to the point (p,q) in the image frame 14-1 using the relationship of Equation (1), reads a color information signal of the point from the picture memory (frame memory) 13-3, and writes the color information signal to an output picture memory (not shown) having an address corresponding to the point (p,q) in the image frame 14-1. Exhibit 1012, [0022-0023].

92. Enami discloses that the parameters for correcting distortion of a fisheye lens image such as a central position of a displayed image, an aspect ratio of the fisheye lens image, and a radius of a fisheye lens image area are extracted from the captured fisheye lens image itself and distortion of the fisheye lens image is corrected using the parameters. Exhibit 1012, [0033].

X. Claim 10 Of The ‘990 Patent Would Have Been Obvious To A Person Of Ordinary Skill In The Art Over Nagaoka In View Of Shiota

93. The Feinberg Declaration (Exhibit 1013) explains how Nagaoka (Exhibit 1003) discloses all the elements of claim 1, *i.e.*, a panoramic objective lens having an image point distribution function that is not linear relative to the

field angle of object points of the panorama, the distribution function having a maximum divergence of at least $\pm 10\%$ compared to a linear distribution function, such that the panoramic image obtained has at least one substantially expanded zone and at least one substantially compressed zone. Feinberg Dec. (Exhibit 1013) ¶¶ 70-115.

94. Nagaoka discloses that the obtained image is “converted into a plane image by the image data processing unit 3,” (Exhibit 1003, col. 8, lines 2-3), but does not disclose the specific correction applied by the image data processing unit. A person of ordinary skill in the art would have recognized that the images obtained using the non-linear lenses in Nagaoka need to be corrected.

95. Shiota discloses correcting the non-linearity of the initial image, performed by means of the non-linear distribution function. Exhibit 1008, [0030-0032].

96. Shiota discloses: “An image is transformed as follows. The projecting position on the image pickup face (p, q coordinates) of a point (u, v coordinates) on a plane image is obtained by arithmetic operation.” Exhibit 1008, [0024].

97. Shiota discloses that the non-linear distribution function $h=2f \cdot \tan(\theta/2)$ is used to compute the coefficient k_2 . $k_2=h/r$, where h is the lens function and r is the distance from the origin. Exhibit 1008, [0037-0042]. Shiota discloses that the

coefficient k_2 is used to obtain the image points that will be displayed. Exhibit 1008, [0031-0035].

98. As the coefficient k_2 used to correct the image is computed using the non-linear distribution function h , Shiota teaches “correcting the non-linearity of the initial image, performed ... by means of the non-linear distribution function.” Exhibit 1008, [0037 and 0040].

99. It would have been obvious to a person of ordinary skill in the art to correct the non-linearity of an initial image obtained using a lens disclosed in Nagaoka with the correction method disclosed in Shiota. Nagaoka teaches obtaining a non-linear image and Shiota discloses correcting the non-linearity of the image by means of the non-linear distribution function.

100. It would further have been obvious to a person of ordinary skill in the art to correct an image obtained using a lens having a non-linear distribution function $h=2f \cdot \tan(\theta/2)$ as disclosed in Nagaoka with a correction method disclosed in Shiota because the non-linear distribution function $h=2f \cdot \tan(\theta/2)$ is used in the correction method disclosed in Shiota. In other words, it would have been obvious to correct an image obtained using a lens having a distribution function $h=2f \cdot \tan(\theta/2)$ with a correction method which uses the same distribution function $h=2f \cdot \tan(\theta/2)$.

101. In view of the above, Shiota discloses all the elements stated in claim 10 of the '990 patent.

102. Claim 10 of the '990 patent would have been obvious to a person of ordinary skill in the art over Nagaoka in view of Shiota.

XI. Claim 10 Of The '990 Patent Would Have Been Obvious To A Person Of Ordinary Skill In The Art Over Nagaoka In View Of Matsui

103. Claim 10 of the '990 patent would have been obvious over Nagaoka in combination with Matsui. As noted earlier, Nagaoka discloses that the obtained image is "converted into a plane image by the image data processing unit 3," (Exhibit 1003, col. 8, lines 2-3), but does not disclose the specific correction applied by the image data processing unit. A person of ordinary skill in the art would have recognized that the images obtained using the non-linear lenses in Nagaoka need to be corrected.

104. Matsui discloses correcting the non-linearity of the initial image, performed by means of the non-linear distribution function. Exhibit 1010, [0025].

105. Matsui discloses a data image conversion device, in which image data obtained with a fish-eye lens is corrected to remove distortion so that it may be displayed. Exhibit 1010, [0001].

106. Matsui discloses that the non-linear lens distribution function $h = 2f \cdot \tan(\theta/2) = 2f \cdot \{\sin\theta/(1 + \cos\theta)\}$. Exhibit 1010, [0025].

107. Matsui discloses the calculation of pixel positions on the circular surface from the pixel positions actually captured by the CCD utilizing the non-linear distribution function $h = 2f \cdot \tan(\theta/2)$. Exhibit 1010, [0025].

108. A data converter 2 that calculates the circular surface S pixel position corresponding to each pixel on the post-conversion cylindrical surface C, then converts the pixel data of the pixel positions as respective pixel data on the cylindrical surface C. As a result, as shown in Fig. 4, the pixel data on the circular surface S is converted as respective pixel data on the cylindrical surface C. Exhibit 1010, [0026].

109. The data converter 2 converts P1 shown in Fig. 3 into P2 shown in Fig. 2. Exhibit 1010, [0023].

110. Matsui additionally discloses correcting the non-linearity of the initial image by means of the reciprocal of the non-linear lens distribution function. Exhibit 1010, [0030-0031].

111. Specifically, Matsui discloses that rather than using the lens distribution function $h = g(\theta)$, an inverse function $\theta = \tan^{-1}(R/z)$ can be used to relate points on the cylindrical surface to the points in the circular image. In this case, the points in the circular image can be directly referenced by indexing ψ and z of the cylindrical coordinates according to the relationship $(f \cdot G(\tan^{-1}(R/z)) \cdot \cos\psi, f \cdot G(\tan^{-1}(R/z)) \cdot \sin\psi)$. Exhibit 1010, [0030-0031].

112. It would have been obvious to a person of ordinary skill in the art to correct an image obtained from the lens described in Nagaoka with the correction method disclosed in Matsui.

113. It would further have been obvious to a person of ordinary skill in the art to correct an image obtained using a lens having a non-linear distribution function $h=2f \cdot \tan(\theta/2)$ as disclosed in Nagaoka with a correction method where the non-linear distribution function $h=2f \cdot \tan(\theta/2)$ is used in the correction method, as disclosed in Matsui. In other words, it would have been obvious to correct an image obtained using a lens having a distribution function $h=2f \cdot \tan(\theta/2)$ with a correction method which uses the same distribution function $h=2f \cdot \tan(\theta/2)$.

114. In view of the above, Matsui discloses all the elements stated in claim 10 of the '990 patent.

115. Claim 10 of the '990 patent would have been obvious to a person of ordinary skill in the art over Nagaoka in view of Matsui.

XII. Claim 11 Of The '990 Patent Would Have Been Obvious To A Person Of Ordinary Skill In The Art Over Nagaoka In View Of Shiota

116. Shiota discloses a stereoscopic projection having a relationship $h=2f \cdot \tan(\theta/2)$, which produces an image having an expanded portion. Exhibit 1008, [0037].

117. Shiota further discloses that the position of a pixel on the fish-eye image will not necessarily map to a pixel on the plane image and hence nearby pixels would be used for interpolation. Exhibit 1008, [0049].

118. Because Shiota has an expanded portion, a person of ordinary skill in the art would have known that the number of image points in a corrected digital image would be larger than the number of points in the initial image. Considering a region in the initial image that is to be expanded, each initial image point will represent the projection of multiple spatial points according to the lens system. Hence, during the expansion process, the image points will be mapped to one or more points in the corrected digital image. Shiota discloses this step of transforming the initial image into a corrected digital image where the number of image points is higher than the number of pixels of the image sensor.

119. It would have been obvious to a person of ordinary skill in the art to correct the non-linearity of an initial image obtained using a lens disclosed in Nagaoka with the correction method disclosed in Shiota. Shiota discloses correcting the non-linearity of the initial image by means of the non-linear distribution function. Exhibit 1008, [0037].

120. It would have also been obvious to correct the non-linearity of an initial image obtained using the Nagaoka lens, which has a non-linear distribution function $h=2f \cdot \tan(\theta/2)$, with the correction method disclosed in Shiota, which uses

the non-linear distribution function $h=2f \cdot \tan(\theta/2)$ to correct the initial image.

When Nagaoka and Shiota are so combined, the initial image is necessarily transformed into a corrected digital image comprising a number of image points higher than the number of pixels of the image sensor. Exhibit 1008, [0037].

121. In view of the above, Shiota discloses all the elements stated in claim 11 of the '990 patent.

122. Claim 11 of the '990 patent would have been obvious to a person of ordinary skill in the art over Nagaoka in view of Shiota.

XIII. Claims 15 And 16 Of The '990 Patent Would Have Been Obvious To A Person Of Ordinary Skill In The Art Over Nagaoka In View Of Shiota And In Further View Of Enami

123. Enami discloses the color allocation stated in claim 15.

124. It would have been obvious to a person of ordinary skill in the art to allocate the colors of the image obtained using Nagaoka and corrected using Shiota with the color allocation taught in Enami as it would ensure that the mapped coordinates are assigned the appropriate color value and provide a more accurate corrected image.

125. Enami discloses that the image img captured by the fisheye lens camera may be regarded as mapping of an image incident from a specific direction (r, θ, ϕ) to a point (x'', y'') expressed by a mapping transformation of Equation (2) in the two-dimensional x-y plane. In Equation (2), θ indicates an azimuth angle, ϕ

indicates a vertex angle (zenith angle), and L indicates a distance (image height) from the origin O when an image incident at the vertex angle ϕ is formed on a fisheye lens image” Exhibit 1012, [0053].

126. Enami discloses that the fisheye lens image img may be considered as mapping to two-dimensional (x'', y'') from a point of the three-dimensional coordinate (r, θ, ϕ). The distance (image height) L is different depending on a projection formula of the fisheye lens, and is expressed as in Equation (3-1)”. Exhibit 1012, [0055].

127. Equation 3-2, reproduced below, is a non-linear distribution function:

$$L = 2f \sin \frac{\phi}{2}$$

128. Enami discloses determining the color of image points of a display window, by projecting the image points of the display window onto the initial image by means of the non-linear distribution function. Exhibit 1012, [0058].

129. Enami discloses allocating to each image point of the display window the color of an image point that is the closest on the initial image. Exhibit 1012, [0072-0074]. In doing so, Enami specifically discloses finding the closest coordinate point on the fisheye lens image as the first step by converting mapped coordinate points to integers by omitting the decimal points, and utilizing the color values at the corresponding integer coordinate points. Similarly, rounding up to

obtain the closest point or the integer coordinate is also disclosed. Finally, the use of both integer coordinates is disclosed as part of linear interpolation. It would have been well understood by a person of ordinary skill in the art that the use of closest point constitutes a form of interpolation and multiple approaches could be utilized in determining the closest point, one such approach being disclosed by Enami. Exhibit 1012, [0072-0074].

130. Enami discloses a coordinate of a point of the fisheye lens image *img* corresponding to a coordinate of each point arranged on a raster in the image frame *frm* is specified, and a color information signal of the point having the coordinate is made to correspond to a color information signal of a point having a coordinate of the display frame *frm*, and thus it is possible to perform a correction process of transforming the fisheye lens image *img* to an original image. Exhibit 1012, [0058].

131. Enami discloses that the point (x'' , y'') of the fisheye lens image obtained through the above-described operation is indicated by the coordinate point (u , v). In order to smoothly interpolate this coordinate point (u , v), the following interpolation process is performed. Color information signal components of three colors of a picture signal are indicated by Y , U , and V , those components of the point (u , v) are indicated by $Y_{u, v}$, $U_{u, v}$, and $V_{u, v}$, values which become an integer by omitting decimal points of the coordinate components

u and v of the point (u, v) are indicated by u_0 and v_0 , and a value of the color information signal Y in a point having the coordinate (u_0, v_0) is indicated by $Y_{u_0v_0}$. Similarly, the same content is indicated by $U_{u_0v_0}$ and $V_{u_0v_0}$ for the color information signals U and V. In addition, values obtained by rounding up decimal points of the coordinate components u and v are respectively indicated by u_1 and v_1 , and values of the color information signals Y, U and V having a coordinate corresponding thereto are respectively indicated by $Y_{u_1v_1}$, $U_{u_1v_1}$, and $V_{u_1v_1}$. Further, decimal parts of the coordinate components u and v are respectively indicated by du and dv . Exhibit 1012, [0072].

132. Enami discloses the projection of the image points of the display window onto the initial image comprises projecting the image points of the display window onto a sphere or a sphere portion. Exhibit 1012, [0065-0066].

133. Enami discloses mapping from a three-dimensional coordinate point (x, y, z) to a point P (x'' , y'') of the fisheye lens image on the two-dimensional coordinates is first performed by transforming the point (x, y, z) into a point (r, θ , ϕ) expressed in polar coordinates. This transform can be performed using a polar coordinate transform expression of Equation (5). Exhibit 1012, [0066].

134. Enami discloses determining the angle in relation to the center of the sphere or the sphere portion of each projected image point. Exhibit 1012, [0080-0083].

135. Enami discloses that a transform can be performed using a polar coordinate transform expression of Equation (5).

$$\left. \begin{aligned} r &= \sqrt{x^2 + y^2 + z^2} \\ \theta &= \tan^{-1}(x/y) = \cos^{-1}(x/\sqrt{x^2 + y^2}) \\ \phi &= \cos^{-1}(z/r) = \tan^{-1}(\sqrt{x^2 + y^2}/z) \end{aligned} \right\} \dots(5)$$

Exhibit 1012, [0067].

136. Enami discloses projecting onto the initial image each image point projected onto the sphere or the sphere portion. Exhibit 1012, [0070-0071].

137. Enami discloses a fisheye lens of an equal area mapping formula is expressed by an expression of Equation (3-2), and this equation is assigned to Equation (2) so as to obtain an expression of Equation (6). The expression of Equation (5) is simplified to the expression of Equation (7), as shown below, using the relations $x^2 + y^2 + z^2 = x'^2 + y'^2 + z'^2 = r^2$, and basic trigonometric geometry.

$$\left. \begin{aligned} u &= \frac{\sqrt{2}fx\sqrt{r-z}}{\sqrt{r}\sqrt{x^2+y^2}} = \frac{\sqrt{2}fx\sqrt{r-z}}{\sqrt{r}\sqrt{r^2-z^2}} = \frac{\sqrt{2}fx}{\sqrt{r(r+z)}} \\ v &= \frac{fy\sqrt{r-z}}{\sqrt{r}\sqrt{x^2+y^2}} = \frac{fy\sqrt{r-z}}{\sqrt{r}\sqrt{r^2-z^2}} = \frac{\sqrt{2}fy}{\sqrt{r}\sqrt{r(r+z)}} \end{aligned} \right\} \dots(7)$$

Exhibit 1012, [0068].

138. Enami discloses the projection being performed by means of the non-linear distribution function considering the field angle that each point to be projected has in relation to the center of the sphere or the sphere portion. Exhibit

1012, [0084-0085]. The field angle is defined according to the horizontal and vertical extents in the image area while the center is defined to be the image center position. Exhibit 1012, [0081-0082].

139. Enami discloses a fisheye lens of an equal area mapping formula is expressed by an expression of Equation (3-2), and this equation is assigned to Equation (2) so as to obtain an expression of Equation (6). Exhibit 1012, [0068].

140. Accordingly, Enami teaches allocating to each image point of the display window the color of an image point that is the closest on the initial image.

141. It would have been obvious to a person of ordinary skill in the art to correct an image obtained from the lens described in Nagaoka with the corrections disclosed in Shiota and Enami.

142. Shiota also discloses the element stated in claim 16.

143. Shiota also discloses that the plane image is generated by referring to the luminance information of the points in the fish-eye image. Exhibit 1008, [0024].

144. Shiota discloses “transforming a fisheye image obtained using a fisheye lens (2) into a plane image for display comprising: a first coordinate calculating unit (35) for obtaining first projection coordinates derived by projecting coordinates on the plane image onto a fisheye face as an imaginary object face.” Exhibit 1008, Abstract.

145. Shiota discloses “Necessary parameters are, as shown in Figs. 1 and 2, (X_0, Y_0, Z_0) indicative of the center (origin) of a plane image and change amounts $\partial u_x, \partial v_x, \partial u_y, \partial v_y, \partial u_z, \partial v_z$ in the respective axes of the (X, Y, Z) coordinates when a point is moved in the respective directions on the (u, v) coordinate system by an amount of one pixel (corresponding to one pixel on the monitor screen). Exhibit 1008 [0025]. “The parameters can be easily obtained from the information of the angle information (ψ, θ, α) of the view point and the magnification of the image.” Exhibit 1008, [0026]. Since point P’ “is on the surface of the hemisphere of radius of 1, the zenithal angle (θ_1) is unconditionally determined ...” Exhibit 1008, [0034].

146. Shiota discloses “First, the coordinates of a point P’ (first projection coordinates) on the hemispherical face as an imaginary object face, which is a projection of a point P on a plane image (the u, v coordinates) are obtained.” Exhibit 1008, [0028].

147. Shiota discloses as a second step of the calculation, “a procedure of obtaining second projection coordinates $w(p_1, q_1)$ on a fisheye image face from the first projection coordinates (X_2, Y_2, Z_2) determined (refer to FIG. 1 with respect to w) will be explained.” Exhibit 1008, [0033].

148. An example of a specific function of $F(\theta_1)$ according to the projecting method is the stereographic projection, which has the non-linear distribution function: $2f \cdot \tan(\theta/2)$. Exhibit 1008, [0037].

149. After correcting the non-linearity of the initial image using Shiota, it would have been obvious to a person of ordinary skill in the art to allocate the colors of the image with the color allocation taught in Enami as it would ensure that the mapped coordinates are assigned the appropriate color value and provide a more accurate corrected image.

150. It would have been obvious to a person of ordinary skill in the art to correct an image obtained from the lens described in Nagaoka with the corrections disclosed in Shiota and Enami. It would further have been obvious to a person of ordinary skill in the art to also use the projection of the image points of the display window onto the initial image also disclosed in Shiota and Enami to ensure what is in the display window is an image that has uniform resolution across all of its points, and thus provide a more accurate corrected image.

151. In view of the above, Enami discloses all the elements stated in claim 15 of the '990 patent.

152. Enami also discloses all the elements stated in claim 16 of the '990 patent.

153. Additionally, Shiota discloses all the elements stated in claim 16 of the '990 patent.

154. Claims 15 and 16 of the '990 patent would have been obvious to a person of ordinary skill in the art over Nagaoka in view of Shiota and in further view of Enami.

155. Baker can be substituted for Nagaoka and combined with Shiota and Enami. Baker recognizes that “any appropriate corrections” can be made with the image transform processors. Exhibit 1002, 12:51-55. For the same reasons that Nagaoka in view of Shiota render claims 10 and 11 unpatentable (*see* paragraphs 96-102, 116-122 above) and Nagaoka in view of Shiota and in further view of Enami render claims 15 and 16 unpatentable (*see* paragraphs 123-154 above), Baker can be substituted for Nagaoka in each of these combinations thereby rendering claims 10, 11, 15 and 16 unpatentable.

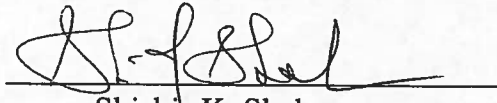
I reserve the right to supplement my opinions in the future to respond to any arguments that Patentee raises and to take into account new information as it becomes available to me.

I declare that all statements made herein of my own knowledge are true and that all statements made on information and belief are believed to be true; and further that these statements were made with the knowledge that willful false

statements and the like so made are punishable by fine or imprisonment, or both,
under Section 1001 of Title 18 of the United States Code.

I declare under penalty of perjury that the foregoing is true and correct.

Aug 13, 2014
Date:


Shishir K. Shah

APPENDIX A

Appendix A

Shishir K. Shah

**2302 Oak Links Avenue
Houston, TX 77059**

Education

Ph.D. Electrical and Computer Engineering, The University of Texas at Austin, 1998

M.S. Electrical and Computer Engineering, The University of Texas at Austin, 1995

B.S. Mechanical Engineering, The University of Texas at Austin, 1994

Appointments

Associate Professor	2010–Present
Department of Computer Science	University of Houston, Houston, TX

Associate Professor	2012–Present
Department of Electrical & Computer Engineering	University of Houston, Houston, TX

Director, Undergraduate Studies	2010–Present
Department of Computer Science	University of Houston, Houston, TX

Director	2005–Present
Quantitative Imaging Laboratory	University of Houston, Houston, TX

Assistant Professor	2005–2010
Department of Computer Science	University of Houston, Houston, TX

President	2003–2005
Spin Diagnostics, Inc.	Houston, TX

President	2000–2002
Spectral Genomics, Inc.	Houston, TX

Projects Manager	1999–2000
BioDiscovery, Inc.	Los Angeles, CA

Assistant Professor	1998–2000
Department of Electrical and Computer Engineering	Wayne State University, Detroit, MI

Graduate Research Assistant	1994–1998
-----------------------------	-----------

Computer and Vision Research Center	The University of Texas at Austin, Austin, TX
Undergraduate Research Assistant	1991–1994
Computer and Vision Research Center/Biomedical Heat Transfer Laboratory	The University of Texas at Austin, Austin, TX

Honors and Awards

Guest Editor	Jan 2012
TBME Letters Special Section on Multiscale Biomedical Signal & Image Modeling & Analysis	
John C. Butler Teaching Excellence Award	2011
College of Natural Science and Mathematics, University of Houston	
Academic Excellence Award	2009
Department of Computer Science, University of Houston	
Associate Editor	2011–Present
IEEE Transactions on Biomedical Engineering	
Editorial Board Member	2008–Present
Journal on Image and Vision Computing	
Professional Development Activities Co-Chair	2013
Biometrics: Theory, Applications and Systems (BTAS)	
Program Committee	2013
The 6th IAPR International Conference on Biometrics	
Session Co-Organizer	2013
10th IEEE Conference on Automatic Face and Gesture Recognition: Special Session on FG in Medicine	
Program Committee	2013
SPIE Defense, Security, and Sensing: Biometric and Surveillance Technology for Human and Activity Identification X	
Program Committee	2013
3D Face Biometrics (In conjunction with FG 2013)	
Program Committee	2012–2013
International Conference on 3D Converged IT and Optical Communications	
Program Committee	2011–2013

International Conference on Ambient Computing, Applications, Services and Technologies

Program Committee 2010

First International Workshop on Computer Vision for Computer Games

International Program Committee 2010

IEEE Conference on Systems, Man, and Cybernetics

Technical Program Committee 2009, 2010

IEEE International Symposium on Biomedical Imaging

Tutorials and Workshops

Digital Image Processing. Five day workshop associated with the Indo-US Collaboration on Engineering Education, Punjab, India, June 2012.

3D-Aided Face Recognition. Half day tutorial at the International Joint Conference on Biometrics, Washington, D.C., October 2011.

Advances in Computer Vision. Five day workshop associated with the Indo-US Collaboration on Engineering Education, Andhra Pradesh, India, July 2011.

Image Computing and Digital Pathology. Full day tutorial at the International Conference on Pattern Recognition, Tampa, FL, December 2008.

Invited Presentations

Social Cues in Modeling Local Human Behavior and its Utility in Human Motion Understanding. Indian Institute of Technology, Gandhinagar, India, March 2013.

Wide Area Surveillance in Distributed Camera Networks. Sardar Vallabhbhai National Institute of Technology, Surat, India, August 2011.

Adaptive Framework for Robust Object Tracking in Dynamic Environments. Institute of Information and Communication Technology, India, December 2009.

Optimal Image Segmentation within a Predictive Framework. Image Sciences, Computer Sciences and Remote Sensing Laboratory, University of Strasbourg, France, January 2009.

Automated Cell Segmentation and Computer-Aided Tool for Fast Screening of Thyroid Fine Needle Aspiration Cytology Smears. Workshop on Computational Surgery and Dual Training, Strasbourg, France, December, 2008.

Image Registration in Medical Imaging. Texas Instruments Medical Imaging Summit, Dallas, TX, April 2008.

Distributed Tracking for Surveillance. Texas Instruments, Dallas, TX, April 2008.

Learning Systems in Computer Vision. ECE Seminar Series, The University of Texas at Austin, Austin, TX, March 2008.

Multispectral Imaging and Automated Analysis for Cytopathology. Symposium on Digital Life Technologies, Tainan, Taiwan, June 2007.

Automatic Cell Image Segmentation using a Shape-Classification Model. Colloquium on Mathematics in Images, University of La Rochelle, France, May 2007.

Automated Cell Segmentation for Cancer Cytology. Third Annual Workshop on Interdisciplinary Computational Science, University of Houston, TX, March 2007.

Internuclei Quantitation. Research Seminar, The Methodist Hospital, Houston, TX, July 2006.

Entrepreneurship and Research: A Perspective. Research Experience for Undergraduates Seminar, University of Houston, Houston, TX, July 2006.

Microscopic Image Analysis. Emerging Researchers Forum, The Methodist Hospital, Houston, TX, May 2006.

Virtual Microscopy and High Performance Computing. University of Houston High Performance Computing Workshop, Houston, TX, March 2006.

Multispectral Imaging for Particle Characterization. Research Seminar, Advanced Digital Imaging Research, LLC., League City, TX, February 2006.

Quantitative Imaging. Graduate Student Seminar, University of Houston, Houston, TX, October 2005.

Differential Thyroid Cytology. Research Seminar, The University of Texas Medical Branch, Galveston, TX, July 2005.

High Throughput Imaging: Approaches and Applications in Biomedical Sciences. Research Seminar, The University of Texas Health Sciences, Houston, TX, June 2005.

Genomic FISHing: Chromosomal Abnormality Screening Using DNA Arrays. Research Seminar, Houston Community College: Biotechnology Program, Houston, TX, April 2005.

Select Publications

Books and Book Articles

1. **S. K. Shah** and A. Gala, **Person Re-identification in Wide Area Camera Networks**, *Augmented Vision and Reality*, Springer, 2013.
2. E. Gabriel, R. Smaoui, V. Venkatesan and **S. K. Shah**, **Hardware and Performance Considerations for Computational Medicine**, *Computational Surgery and Dual Training: Computing, Robotic and Imaging for the Surgery Platform*, Eds. M. Garbey and R. Tran-Son-Tay, Springer, 2013.
3. X. Wu, **S. K. Shah** and F Merchant, **Automated Prototype Generation for Multi-color Karyotyping**, *Color Medical Image Analysis*, Eds. M. Emre Celebi and Gerald Schaefer, Springer, 2013.
4. I.A. Kakadiaris, G. Passalis, G. Toderici, E. Efraty, P. Perakis, D. Chu, **S.K. Shah** and T. Theoharis, **Face Recognition Using 3D Images**, *Handbook of Face Recognition*, Eds. Stan Z. Li and Anil K. Jain, Springer-Verlag, 2011.

5. I. A. Kakadiaris and **S. K. Shah**, **Biomedical Computing in Complex Advanced Systems, Pumps and Pipes**, Eds. M. G. Davies *et al.*, Springer, 2011.
6. **S. K. Shah** and E. Gabriel, **Parallel Multispectral Image Segmentation for Computer Aided Thyroid Cytology**, *Computational Surgery and Dual Training*, Eds. M. Garbey and R. Tran-Son-Tay, Springer, 2010.
7. E. Gabriel and **S. K. Shah**, **Parallelizing Image Analysis Applications for Spectral Microscopy**, *Multivariate Image Processing: Methods and Applications*, Eds. J. Chanussot, K. Chehdi, and C. Collet, Springer Verlag, 2009.
8. J. Thigpen and **S. K. Shah**, **Spectral Imaging, Microscope Image Processing**, Academic Press, 2008.
9. F. Merchant, **S. K. Shah**, and K. Castleman, **Object Measurement, Microscope Image Processing**, Academic Press, 2008.
10. **Microarray Image Analysis - Nuts and Bolts. S. K. Shah** and G. Kamberova, DNA Press, 2002.

Refereed Journal Papers

11. B. Soibam, **S. K. Shah**, G. H. Gunaratne, and G. W. Roman, Modeling Novelty Habituation During Exploratory Activity in Drosophila, *Behavioural Processes*, vol. 97, pp. 63–75, 2013.
12. O. Ocegueda, T. Fang, **S. K. Shah** and I. A. Kakadiaris, 3D-Face Discriminant Analysis using Gauss-Markov Posterior Marginals, *IEEE Trans. Pattern Analysis and Machine Intelligence*, vol. 35-3, pp. 728–739, 2013.
13. B. Soibam, R. L. Goldfeder, C. Manson-Bishop, R. Gamblin, S. D. Pletcher, **S. K. Shah**, G. H. Gunaratne, G. W. Roman, Modeling Drosophila Positional Preferences in Open Field Arenas with Directional Persistence and Wall Attraction, *PLoS One*, vol. 7-10, pp. e46570, 2012.
14. T. Fang, X. Zhao, O. Ocegueda, **S. K. Shah**, and I.A. Kakadiaris, 3D/4D Facial Expression Analysis: An Advanced Annotated Face Model Approach, *Image and Vision Computing*, vol. 30- 10, pp. 738–749, 2012.
15. A. Bedagkar-Gala and **S. K. Shah**, Part-based Spatio-temporal Model for Multi-Person Re-identification, *Pattern Recognition Letters*, vol. 33-14, pp. 1908–1915, 2012.
16. K. Tran, I. A. Kakadiaris, and **S. K. Shah**, Modeling Motion of Body Parts for Action Recognition, *Pattern Recognition*, vol. 45-7, pp. 2562–2572, 2012.
17. X. Wu and **S. K. Shah**, Embedding Topic Discovery in Conditional Random Fields Model for Segmenting Nuclei Using Multispectral Data, *IEEE Trans. Biomedical Engineering*, vol. 59-6, pp. 1539–1549, 2012.

18. B. Efraty, E. Bilgazyev, **S. Shah**, and I.A. Kakadiaris, Profile-based 3D-Aided Face Recognition, *Pattern Recognition*, vol. 45-1, pp. 43–53, 2012.
19. J. Thigpen and **S. Shah**, Photometric Calibration for Quantitative Spectral Microscopy under Transmitted Illumination, *Journal of Microscopy*, vol. 239-3, pp. 200–214, 2010.
20. E. Gabriel, V. Venkatesan, and **S. Shah**, Towards High Performance Cell Segmentation in Multispectral Fine Needle Aspiration Cytology of Thyroid Lesions, *Computer Methods and Programs in Biomedicine*, vol. 98-3, pp. 231–240, 2010.
21. **S. Shah**, Performance Modeling and Algorithm Characterization for Robust Image Segmentation, *International Journal of Computer Vision*, v. 80-1, pp. 92–103, 2008.
22. J. Thigpen, **S. Shah**, and F. Merchant, Cell Differentiation in Multispectral Image Cytology, *Journal of Algorithms and Computational Technology*, v. 2-4, pp. 469–499, 2008.
23. **S. Shah**, Automatic Cell Segmentation using a Shape-Classification Model in Immunohistochemically Stained Cytological Images, *IEICE Transactions on Information and Systems*, v. E91-D-7, pp. 1955–1962, 2008.
24. **S. Shah**, Image Enhancement for Increased Dot-Counting Efficiency in FISH, *Journal of Microscopy*, v. 228-2, pp. 211–226, 2007.
25. T. Man, X. Lu, K. Jaeweon, L. Perlaky, C. Harris, **S. Shah**, M. Ladanyi, R. Gorlick, C. Lau, and P. H. Rao, Genome-wide Array Comparative Genomic Hybridization Analysis Reveals Distinct Amplifications in Osteosarcoma, *BMC Cancer*, 4:45, 2004.

Refereed Conference Papers

26. E. Bilgazyev, U. Kurkure, **S. K. Shah**, and I. A. Kakadiaris, ASIE: application-specific image enhancement for face recognition, in *Proceedings of SPIE Defense, Security, and Sensing*, pp. 87120U–87120U-9, 2013.
27. K. N. Tran, A. Bedagkar-Gala, I. A. Kakadiaris, and **S. K. Shah**, Social Cues in Group Formation and Local Interactions for Collective Activity Analysis, in *Proceedings of 9th International Conference on Computer Vision Theory and Applications*, 2013.
28. X. Zhao, **S. K. Shah**, and I. A. Kakadiaris, Illumination Alignment using Lighting Ratio: Application to 3D-2D Face Recognition, in *Proceedings of 10th IEEE International Conference on Automatic Face and Gesture Recognition*, 2013.
29. D. Chu, **S. K. Shah**, and I. A. Kakadiaris, Face Recognition based on 3D Partial Data using Semi- Coupled Dictionary Learning, in *Proceedings of 10th IEEE International Conference on Automatic Face and Gesture Recognition*, 2013.
30. C. Hans, C. W. McCollum, M. B. Bondesson, J. Gustafsson, **S. K. Shah**, and F. A. Merchant, Automated Analysis of Zebrafish Images for Screening Toxicants, in *Proceedings of 35th Annual International Conference of the IEEE Engineering in Medicine and Biology Society*, 2013.

31. C. Huang, B. A. Efraty, U. Kurkure, M. Papadakis, **S. K. Shah**, and I. A. Kakadiaris, Facial Landmark Configuration for Improved Detection, in *Proceedings of IEEE International Workshop on Information Forensics and Security (WIFS)*, pp. 13–18, 2012.
32. H. Haberdar and **S. K. Shah**, Video synchronization as One-class Learning, in *Proceedings of the 27th Conference on Image and Vision Computing New Zealand*, pp. 469–474, 2012.
33. X. Yan, X. Wu, I. A. Kakadiaris and **S. K. Shah**, To Track or To Detect? An Ensemble Framework for Optimal Selection, in *Proceedings of European Conference on Computer Vision*, pp. 594– 607, 2012.
34. X. Zhao, **S. K. Shah** and I. A. Kakadiaris, Illumination Normalization using Self-lighting Ratios for 3D2D Face Recognition, *Proceedings of European Conference on Computer Vision (Workshop)*, pp. 220-229, 2012.
35. J. Lee, T. Feng, W. Shi, A. Bedagkar-Gala, **S. K. Shah**, and H. Yoshida, Towards Quality Aware Collaborative Video Analytic Cloud, in *Proceedings of IEEE 5th International Conference on Cloud Computing*, pp. 147–154, 2012.
36. T. Tuna, J. Subhlok, L. Barker, V. Varghese, O. Johnson, and **S. K. Shah**, Development and Evaluation of Indexed Captioned Searchable Videos for STEM Coursework, in *Proceedings of SIGCSE: ACM Technical Symposium on Computer Science Education*, pp. 129–134, 2012.
37. T. Tuna, **S. K. Shah**, and J. Subhlok, Indexing and Keyword Search to Ease Navigation in Lecture Videos, in *Proceedings of the Applied Imagery Pattern Recognition Workshop*, pp. 1–8, 2011.
38. M. Amer, E. Bilgazyev, S. Todorovic, **S. K. Shah**, I. A. Kakadiaris, and L. Ciannelli, Fine-grained Categorization of Events in Underwater Videos by Tracking Fish, in *Proceedings of the 3rd International Workshop on Video Event Categorization, Tagging and Retrieval for Real-World Applications (in conjunction with ICCV)*, 2011.
39. T. Fang, X. Zhao, **S. K. Shah** and I. A. Kakadiaris, 4D Facial Expression Recognition, in *Proceedings of IEEE International Conference on Computer Vision (Workshop)*, pp. 1594–1601, 2011.
40. O. Ocegueda, T. Fang, **S. K. Shah** and I. A. Kakadiaris, Expressive Maps for 3D Facial Expression Recognition, in *Proceedings of IEEE International Conference on Computer Vision (Workshop)*, pp. 1270–1275, 2011.
41. B. Efraty, C. Huang, **S. K. Shah**, and I. A. Kakadiaris, Facial Landmark Detection in Uncontrolled Conditions, in *Proceedings of International Joint Conference on Biometrics*, pp. 1–8, 2011.
42. V. Vijayan, K. Bowyer, P. Flynn, D. Huang, L. Chen, M. Hansen, O. Ocegueda, **S. K. Shah**, I. A. Kakadiaris, Twins 3D Face Recognition Challenge, in *Proceedings of International Joint Conference on Biometrics*, pp. 1–7, 2011.

43. E. Bilgazyev, B. Efraty, **S.K. Shah**, and I.A. Kakadiaris, Improved Face Recognition Using Super- Resolution, in *Proceedings of International Joint Conference on Biometrics*, pp. 1–7, 2011.
44. O. Ocegueda, G. Passalis, T. Theoharis, **S. K. Shah**, and I.A. Kakadiaris, UR3D-C: Linear Dimensionality Reduction for Efficient 3D Face Recognition, in *Proceedings of International Joint Conference on Biometrics*, pp. 1–6, 2011.
45. E. Bilgazyev, B. Efraty, **S.K. Shah**, and I.A. Kakadiaris, Sparse Representation-Based Super Resolution for Face Recognition At a Distance, in *Proceedings of British Machine Vision Conference*, pp. 52.1–52.11, 2011.
46. K. N. Tran, I. A. Kakadiaris and **S. K. Shah**, Modeling Motion of Body Parts for Action Recognition, in *Proceedings of British Machine Vision Conference*, pp. 64.1–64.12, 2011.
47. X. Yan, I. A. Kakadiaris and **S. K. Shah**, Predicting Social Interactions for Visual Tracking, in *Proceedings of British Machine Vision Conference*, pp. 102.1–102.11, 2011.
48. C. Hans, A. Shete, **S. K. Shah**, C. W. McCollum, M. B. Bondesson, and F. A. Merchant, 3D Imaging for Quantitative Assessment of Toxicity on Vascular Development in Zebrafish, in *Proceedings of 33rd Annual International Conference of the IEEE Engineering in Medicine and Biology Society*, pp. 5969–5972, Boston, 2011.
49. A. Bose, **S. K. Shah**, G. P. Reece, M. A. Crosby, E. K. Beahm, M. C. Fingeret, M. K. Markey, and F. A. Merchant, Automated Spatial Alignment of 3D Torso Images, in *Proceedings of 33rd Annual International Conference of the IEEE Engineering in Medicine and Biology Society*, pp. 8455–8458, Boston, 2011.
50. B. Efraty, M. Papadakis, A. Profitt, **S. K. Shah** and I.A. Kakadiaris, Pose invariant facial Component-landmark detection, in *Proc. of IEEE International Conf. on Image Processing*, pp. 569–572, Belgium, 2011.
51. O. Ocegueda, **S. K. Shah**, and I.A. Kakadiaris, Which parts of the face give out your identity?, in *Proc. IEEE Computer Society Conference on Computer Vision and Pattern Recognition*, pp. 641–648, Colorado Springs, CO, June 20-25, 2011.
52. X. Wu and **S. K. Shah**, Cell Segmentation in Multispectral Images using Level Sets with Priors for Accurate Shape Recovery, in *Proc. IEEE International Symposium on Biomedical Imaging*, pp. 2117–2120, Chicago, 2011.
53. B. Efraty, M. Papadakis, A. Profitt, **S.K. Shah**, and I.A. Kakadiaris, Facial Component Landmark Detection, in *Proc. IEEE International Conference on Automatic Face and Gesture Recognition*, pp. 278–285, Santa Barbara, CA, Mar. 21-23, 2011.
54. E. Bilgazyev, **S.K. Shah**, and I.A. Kakadiaris, Comparative Evaluation of Wavelet based Super- Resolution from Video for Face Recognition at a Distance, in *Proc. IEEE International Conference on Automatic Face and Gesture Recognition*, pp. 559–565, Santa Barbara, CA, Mar. 21-23, 2011.

55. T. Fang, X. Zhao, O. Ocegueda, **S. K. Shah**, and I.A. Kakadiaris, 3D Facial Expression Recognition: A Perspective on Promises and Challenges, in *Proc. IEEE International Conference on Automatic Face and Gesture Recognition*, pp. 603–610, Santa Barbara, CA, Mar. 21-23, 2011.
56. X. Wu and **S. K. Shah**, Level Set with Embedded Conditional Random Fields and Shape Priors for Segmentation of Overlapping Objects, in *Proceedings of Asian Conference on Computer Vision*, pp. 230–241, 2010.
57. Z. Zheng, T. Fang, **S. K. Shah**, and I. A. Kakadiaris, Personalized 3D-Aided 2D Facial Landmark Localization, in *Proceedings of Asian Conference on Computer Vision*, pp. 633–646, 2010.
58. C. Hans, F. A. Merchant, and **S. K. Shah**, Decision Fusion for Urine Particle Classification in Multispectral Images, in *Proceedings of Indian Conference on Computer Vision, Graphics, and Image Processing*, pp. 419–426, 2010.
59. M. Wendt and **S. K. Shah**, Segmentation of Crystalline Lens in Photorefractive Video, in *Proceedings of Indian Conference on Computer Vision, Graphics, and Image Processing*, pp. 322–329, 2010.
60. H. Haberdar and **S. K. Shah**, Disparity Map Refinement for Video Based Scene Change Detection Using a Mobile Stereo Camera Platform, in *Proceedings of 20th International Conference on Pattern Recognition*, pp. 3890–3893, Istanbul, Turkey, 2010.
61. A. Gala and **S. K. Shah**, Joint Modeling of Algorithm Behavior and Image Quality for Algorithm Performance Prediction, in *Proceedings of British Machine Vision Conference*, pp. 31.1–31.11, 2010.
62. K. Tran, I.A. Kakadiaris, and **S.K. Shah**, Fusion of Human Postures for Continuous Action Recognition, in *Workshop on Sign, Gesture, and Activity, European Conference on Computer Vision*, 2010.
63. X. Wu and **S. K. Shah**, A Bottom-Up and Top-Down Model for Cell Segmentation using Multispectral Data, in *Proceedings of IEEE International Symposium on Biomedical Imaging*, pp. 592–595, Rotterdam, The Netherlands, 2010.
64. D. Chittajallu, **S. Shah**, and I. A. Kakadiaris, A Shape-Driven MRF Model for the Segmentation of Organs in Medical Images, in *Proceedings of IEEE International Conference on Computer Vision and Pattern Recognition*, pp. 3233–3240, San Francisco, CA, 2010.
65. X. Wu and **S. Shah**, Malignancy Detection in Fine-Needle Aspiration Biopsy of the Thyroid using Multispectral Microscopy and Bag-of-Features, in *Proceedings of Fourth International Workshop on Microscopic Image Analysis with Applications in Biology*, Bethesda, MD, 2009.

66. X. Wu and **S. K. Shah**, Random Field Model for Cell Segmentation in Transmission Mode Multispectral Microscopy Images, in *Proceedings of the 43rd Asilomar Conference on Signals, Systems and Computers*, pp. 795–798, 2009.
67. B.A. Efraty, D. Chu, E. Ismailov, **S. Shah**, and I.A. Kakadiaris, Towards 3D-Aided Profile-Based Face Recognition, in *Proceedings of IEEE Third International Conference on Biometrics: Theory, Applications and Systems*, pp. 1–8, Washington, DC, 2009.
68. Z. Zeng, T. Fang, **S. Shah**, and I.A. Kakadiaris, Local Feature Hashing for Face Recognition, in *Proceedings of IEEE Third International Conference on Biometrics: Theory, Applications and Systems*, pp. 1–8, Washington, DC, 2009.
69. B. Soibam, A. Chaudhry, J. Eledath, and **S. Shah**, Quantitative Comparison of Metrics for Change Detection for Video Patrolling Applications, in *Proceedings of IEEE International Workshop on Video-Oriented Object and Event Classification*, pp. 601–608, Kyoto, Japan, 2009.
70. P. Viswanath, I.A. Kakadiaris, and **S. Shah**, A Simplified Error Model for Height Estimation using a Single Camera, in *Proceedings of IEEE Ninth International Workshop on Visual Surveillance*, pp. 1259–1266, Kyoto, Japan, 2009.
71. X. Wu and **S. Shah**, A Conditional Random Field Model for Cell Segmentation Using Multispectral Data, in *Proceedings of MICCAI Workshop on Optical Tissue Image analysis in Microscopy, Histopathology and Endoscopy*, pp. 78–87, London, UK, 2009.
72. B.A. Efraty, D. Chu, E. Ismailov, **S. Shah**, and I.A. Kakadiaris, 3D-Aided Profile-based Face Recognition, in *Proceedings of IEEE International Conference on Image Processing*, pp. 4125–4128, Cairo, Egypt, 2009.
73. J. Thigpen, X. Wu, and **S. Shah**, Multispectral Microscopy and Cell Segmentation for Analysis of Thyroid Fine Needle Aspiration Cytology Smears, in *Proceedings of 31st Annual International Conference of the IEEE Engineering in Medicine and Biology Society*, pp. 5645–5648, Minneapolis, MN, 2009.
74. X. Wu and **S. Shah**, A Fast Band Selection Method to Increase Image Contrast for Multispectral Image Segmentation, in *Proceedings of IEEE International Symposium on Biomedical Imaging*, Boston, MA, pp. 1123–1126, 2009.
75. X. Wu and **S. Shah**, Comparative Analysis of Cell Segmentation using Absorption and Color Images in Fine Needle Aspiration Cytology, in *Proceedings of IEEE Conference on Systems, Man, and Cybernetics, Singapore*, pp. 271–276, 2008.
76. X. Wu and **S. Shah**, Automated Cell Segmentation in Absorption Image of Papanicolaou Stained Cell Smears, in *Proceedings of 3rd Workshop on Microscopic Image Analysis with Applications in Biology (in conjunction with MICCAI, NY)*, 2008.
77. E. Gabriel, V. Venkatesan, and **S. Shah**, Towards High Performance Cell Segmentation in Multispectral Fine Needle Aspiration Cytology of Thyroid Lesions, in *Proceedings of 1st*

Workshop on High-Performance Medical Image Computing & Computer Aided Intervention (in conjunction with MICCAI, NY), 2008.

78. J. Thigpen, and **S. Shah**, Multispectral Microscopy for Cell Differentiation in Thyroid Cytology, in *Proceedings of IEEE Conference on Multisensor Fusion and Integration for Intelligent Systems, Seoul, Korea*, pp. 267–271, 2008.
79. J. Thigpen, **S. Shah**, and F. Merchant, Automatic Cell Differentiation using Multispectral Microscopy, in *Proceedings of 11th WSEAS International Conference in Computers, vol. 4*, pp. 616–621, 2007.
80. **S. Shah**, Automatic Cell Segmentation using a Shape-Classification Model, in *Proceedings of IAPR Conference on Machine Vision Applications*, pp. 428–432, 2007.
81. **S. Shah** and F. Merchant, I-FISH: Increasing Detection Efficiency for Fluorescent Dot Counting in Cell Nuclei, in *6th International Conference on Advances in Pattern Recognition, India*, pp. 220–225, 2007.
82. J. Thigpen, **S. Shah**, F. Merchant, and K. Castleman, Photometric Calibration for Automated Multispectral Imaging of Biological Samples, in *Proceedings of 1st Workshop on Microscopic Image Analysis with Applications in Biology (in conjunction with MICCAI, Copenhagen)*, pp. 27–33, 2006.
83. **S. Shah**, Quantitative Analysis of Array CGH, in *Proceedings of Workshop on Challenges in Clinical Oncology (in conjunction with MICCAI, Copenhagen)*, pp. 69–76, 2006.
84. **S. Shah**, Statistical Framework for Quantitative Analysis of Array CGH, *Proceedings of IEEE International Conference of the Engineering in Medicine and Biology Society*, pp. 5806–5809, 2006.
85. J. Thigpen, **S. Shah**, F.A. Merchant, and K. Castleman, Calibrating Multispectral Imaging System for Biological Particle Analysis under Transmitted Illumination, *Proceedings of Microscopy and Microanalysis*, vol. 12-2, pp. 1678–1679, 2006.
86. **S. Shah** and F. A. Merchant, Fluorescence Dot Counting Efficiency in Radiance Mapped Images, *Proceedings of Microscopy and Microanalysis*, vol. 12-2, pp. 1676–1677, 2006.
87. **S. Shah**, Multispectral Integration for Segmentation of Chromosome Images, *Proceedings of 11th International Conference on Computer Analysis of Images and Patterns*, pp. 506–513, France 2005.

Patents and Provisionals

High Throughput Imaging Device and Methods.

Compilations of Nucleic Acids and Arrays and Methods of Using Them.

Methods for Array-based Comparative Binding Assays.

High Throughput Imaging Device and Method (CIP).

Array Comprising Pre-labeled Biological Molecules and Methods for Making and Using These Arrays.

Arrays, Computer Program Products and Methods for In-silico Array-based Comparative Binding Arrays.

Compilations of Nucleic Acids and Arrays and Methods of Using Them (CIP).

Array Comprising Pre-labeled Biological Molecules and Methods for Making and Using These Arrays (CIP).

Methods for Mapping the Chromosomal Loci of Genes Expressed by a Cell.